adjusted error rate (α') for the six subsequent planned pairwise comparisons was 0.009. $n = 8$ PIs for each group.

PIs are distributed normally. Hence, these data were analysed by analysis of variance with subsequent pairwise comparisons adjusted to maintain an experiment-wise error rate of $\alpha = 0.05$. In Fig. 3, the error rate for the one subsequent planned comparison was 0.05. In Fig. 4, to maintain an experiment-wise error rate of $\alpha = 0.05$, the adjusted error rates (α') were $P = 0.004$ and 0.01, respectively, for the 13 subsequent planned pairwise comparisons in Fig. 4a and for the 5 subsequent planned comparisons in Fig. 4b. The number of PIs included in each group mean is listed above the corresponding bar in all figures.

Received 25 January; accepted 28 March 2001.

1. Scoville, W. B. & Milner, B. Loss of recent memory after bilateral hippocampal lesions. *J. Neuropsychiat. Clin. Neurosci.* **12,** 103–113 (2000).
2. Milner, B., Squire, L. R. & Kandel, E. R. Cognitive neuroscience and the study of memory. *Neuron* **20,** 445–468 (1998).
3. Mayford, M. *et al.* Control of memory formation through regulated expression of a CaMKII transgene. *Science* **274,** 1678–1683 (1996).
4. Shimizu, E., Tang, Y. P., Rampon, C. & Tsien, J. Z. NMDA receptor-dependent synaptic reinforcement as a crucial process for memory consolidation. *Science* **290,** 1170–1174 (2000).
5. de Belle, J. S. & Heisenberg, M. Associative odor learning in *Drosophila* abolished by chemical ablation of mushroom bodies. *Science* **263,** 692–695 (1994).
6. Hammer, M. & Menzel, R. Multiple sites of associative odor learning as revealed by local brain microinjections of octopamine in honeybees. *Learn. Mem.* **5,** 146–156 (1998).
7. Kitamoto, T. Conditional modification of behavior in *Drosophila* by targeted expression of a temperature-sensitive *shibire* allele in defined neurons. *J. Neurobiol.* **47,** 81–92 (2001).
8. Rybak, J. & Menzel, R. Anatomy of the mushroom bodies in the honey bee brain: the neuronal connections of the α-lobe. *J. Comp. Neurol.* **334,** 444–465 (1993).
9. Strausfeld, N. J. & Li, Y. Organization of olfactory and multimodal afferent neurons supplying the calyx and pedunculus of the cockroach mushroom bodies. *J. Comp. Neurol.* **409,** 603–625 (1999).
10. Ito, K. *et al.* The organization of extrinsic neurons and their implications in the functional roles of the mushroom bodies in *Drosophila melanogaster* Meigen. *Learn. Mem.* **5,** 52–77 (1998).
11. Connolly, J. B. *et al.* Associative learning disrupted by impaired Gs signaling in *Drosophila* mushroom bodies. *Science* **274,** 2104–2106 (1996).
12. Zars, T., Fischer, M., Schulz, R. & Heisenberg, M. Localization of a short-term memory in *Drosophila*. *Science* **288,** 672–675 (2000).
13. Poodry, C. A., Hall, L. & Suzuki, D. T. Developmental properties of Shibire: a pleiotropic mutation affecting larval and adult locomotion and development. *Dev. Biol.* **32,** 373–386 (1973).
14. Poodry, C. A. & Edgar, L. Reversible alteration in the neuromuscular junctions of *Drosophila melanogaster* bearing a temperature-sensitive mutation, *shibire*. *J. Cell Biol.* **81,** 520–527 (1979).
15. Ramaswami, M., Rao, S., van der Bliek, A., Kelly, R. B. & Krishnan, K. S. Genetic studies on dynamin function in *Drosophila*. *J. Neurogenet.* **9,** 73–87 (1993).
16. Koenig, J. H. & Ikeda, K. Disappearance and reformation of synaptic vesicle membrane upon transmitter release observed under reversible blockage of membrane retrieval. *J. Neurosci.* **9,** 3844–3860 (1989).
17. Chen, M. S. *et al.* Multiple forms of dynamin are encoded by *shibire*, a *Drosophila* gene involved in endocytosis. *Nature* **351,** 583–586 (1991).
18. van der Bliek, A. M. & Meyerowitz, E. M. Dynamin-like protein encoded by the *Drosophila shibire* gene associated with vesicular traffic. *Nature* **351,** 411–414 (1991).
19. Damke, H., Baba, T., Warnock, D. E. & Schmid, S. L. Induction of mutant dynamin specifically blocks endocytic coated vesicle formation. *J. Cell Biol.* **127,** 915–934 (1994).
20. Grant, D., Unadkat, S., Katzen, A., Krishnan, K. S. & Ramaswami, M. Probable mechanisms underlying interallelic complementation and temperature-sensitivity of mutations at the *shibire* locus of *Drosophila melanogaster*. *Genetics* **149,** 1019–1030 (1998).
21. Brand, A. H. & Perrimon, N. Targeted gene expression as a means of altering cell fates and generating dominant phenotypes. *Development* **118,** 401–415 (1993).
22. Yang, M. Y., Armstrong, J. D., Vilinsky, I., Strausfeld, N. J. & Kaiser, K. Subdivision of the *Drosophila* mushroom bodies by enhancer-trap expression patterns. *Neuron* **15,** 45–54 (1995).
23. Joiner, M. A. & Griffith, L. C. Mapping of the anatomical circuit of CaM kinase-dependent courtship conditioning in *Drosophila*. *Learn. Mem.* **6,** 177–192 (1999).
24. Benzer, S. Behavioral mutants of *Drosophila* isolated by countercurrent distribution. *Proc. Natl Acad. Sci. USA* **58,** 1112–1119 (1967).
25. Tully, T., Preat, T., Boynton, S. C. & Del Vecchio, M. Genetic dissection of consolidated memory in *Drosophila*. *Cell* **79,** 35–47 (1994).
26. Wang, Y. T. & Linden, D. J. Expression of cerebellar long-term depression requires postsynaptic clathrin-mediated endocytosis. *Neuron* **25,** 635–647 (2000).
27. Carroll, R. C. *et al.* Dynamin-dependent endocytosis of ionotropic glutamate receptors. *Proc. Natl Acad. Sci. USA* **96,** 14112–14117 (1999).
28. Dudai, Y., Corfas, G. & Hazvi, S. What is the possible contribution of Ca^{2+}-stimulated adenylate cyclase to acquisition, consolidation and retention of an associative olfactory memory in *Drosophila*? *J. Comp. Physiol. A* **162,** 101–109 (1988).
29. Waddell, S., Armstrong, J. D., Kitamoto, T., Kaiser, K. & Quinn, W. G. The amnesiac gene product is expressed in two neurons in the *Drosophila* brain that are critical for memory. *Cell* **103,** 805–813 (2000).
30. Dubnau, J. & Tully, T. Functional anatomy: from molecule to memory. *Curr. Biol.***11,** R240–R243 (2001).

Supplementary information is available on *Nature*'s World-Wide Web site (http://www.nature.com) or as paper copy from the London editorial office of *Nature*.

Acknowledgements

We thank H. Cline, E. Drier, J. Huang, M. Regulski and K. Svoboda for comments on the manuscript. This work was supported by the NIH (J.T.D. and T.T.) and the NSF (T.K.).

Correspondence and requests for materials should be addressed to J.D. (e-mail: dubnau@cshl.org).

Leptin activates anorexigenic POMC neurons through a neural network in the arcuate nucleus

Michael A. Cowley*†, James L. Smart*†, Marcelo Rubinstein‡, Marcelo G. Cerdán‡, Sabrina Diano§, Tamas L. Horvath§‖, Roger D. Cone* & Malcolm J. Low*

* *The Vollum Institute, Oregon Health Sciences University, Portland, Oregon 97201-3098, USA*
‡ *Instituto de Investigaciones en Ingeniería Genética y Biología Molecular, CONICET and Department of Biology, School of Sciences, University of Buenos Aires 1428, Argentina*
§ *Reproductive Neurosciences Unit, Department of Obstetrics and Gynecology and* ‖ *Department of Neurology, Yale Medical School, New Haven, Connecticut 06520, USA*
† *These authors contributed equally to this work*

The administration of leptin[1] to leptin-deficient humans, and the analogous *Lep^{ob}*/*Lep^{ob}* mice, effectively reduces hyperphagia and obesity[2,3]. But common obesity is associated with elevated leptin, which suggests that obese humans are resistant to this adipocyte hormone. In addition to regulating long-term energy balance, leptin also rapidly affects neuronal activity[4–6]. Proopiomelanocortin (POMC) and neuropeptide-Y types of neurons in the arcuate nucleus of the hypothalamus[7] are both principal sites of leptin receptor expression and the source of potent neuropeptide modulators, melanocortins and neuropeptide Y, which exert opposing effects on feeding and metabolism[8,9]. These neurons are therefore ideal for characterizing leptin action and the mechanism of leptin resistance; however, their diffuse distribution makes them difficult to study. Here we report electrophysiological recordings on POMC neurons, which we identified by targeted expression of green fluorescent protein in transgenic mice. Leptin increases the frequency of action potentials in the anorexigenic POMC neurons by two mechanisms: depolarization through a nonspecific cation channel; and reduced inhibition by local orexigenic neuropeptide-Y/GABA (γ-aminobutyric acid) neurons. Furthermore, we show that melanocortin peptides have an autoinhibitory effect on this circuit. On the basis of our results, we propose an integrated model of leptin action and neuronal architecture in the arcuate nucleus of the hypothalamus.

Previous studies suggest that leptin does not have equal effects on all neuronal subtypes. Acute leptin treatment presumably activates POMC, but not neuropeptide Y (NPY) neurons in the arcuate nucleus of the hypothalamus (ARC), because c-Fos protein is increased only in the former population and Socs3 messenger RNA is increased in both[10]. Furthermore, a population of ARC neurons seems to be inhibited directly by leptin, but the peptide phenotype of these neurons has not been directly established[11–14]. In addition to leptin receptors, both POMC and NPY neurons express a receptor, MC3-R, for POMC-derived melanocortin peptides[15]. The physiological role of this receptor is not well understood, although MC3-R null mice have increased adiposity compared with wild-type mice[16].

To test the hypothesis that leptin selectively activates POMC neurons, we first generated a strain of transgenic mice expressing green fluorescent protein (EGFP; Clontech) under the transcriptional control of mouse *Pomc* genomic sequences, including a region located between −13 kilobases (kb) and −2 kb that is required for accurate neuronal expression[17] (Fig. 1a). Bright green fluorescence (509 nm) was seen in the two central nervous system regions where POMC is produced: the ARC and the nucleus of the solitary tract (data not shown).

Under ultraviolet (450–480 nm) excitation, POMC neurons were clearly distinguished from adjacent, non-fluorescent neurons (Fig. 1b) visualized under infrared optics. Double immunofluorescence showed that there was more than 99% cellular colocalization of EGFP and POMC peptides in the ARC (Fig. 1c). There was close apposition of both tyrosine-hydroxylase- and NPY-stained terminals on EGFP-expressing POMC neurons, but no evidence of colocalization of the tyrosine hydroxylase or NPY immunoreactivity with EGFP (data not shown). Total fluorescent cell counts of coronal hypothalamic sections determined that there were 3,148 ± 62 (mean ± s.e.m.; n = 3) POMC-EGFP neurons distributed through the whole ARC[18] (Fig. 1d). POMC neurons are located both medially and ventrally in mouse ARC, in contrast to a predominantly lateral position in rat ARC.

POMC-EGFP neurons in hypothalamic slices had a resting membrane potential of −40 to −45 mV and exhibited frequent spontaneous action potentials. The non-selective opioid agonist met-enkephalin (Met-Enk, 30 μM; Sigma) caused a rapid (35–40 s), reversible hyperpolarization (10–20 mV) of the membrane potential of POMC cells (n = 10) and prevented spontaneous action potential generation (Fig. 2a). In normal (2.5 mM K^+) Krebs solution, the reversal potential of the inwardly rectifying opioid current was about −90 mV, whereas in 6.5 mM K^+ Krebs solution the reversal potential shifted to about −60 mV (n = 3; Fig. 2b). The μ-opioid receptor (MOP-R) antagonist CTAP (1 μM; Phoenix Pharmaceuticals) completely prevented the current induced by Met-Enk in POMC cells (n = 3; Fig. 2c). These characteristics indicate that the opioid current was caused by both activation of MOP-R and increased ion conductance through G-protein-coupled, inwardly rectifying potassium channels[19]. The similarity of opioid responses in EGFP-labelled POMC neurons to those of guinea-pig[19] or

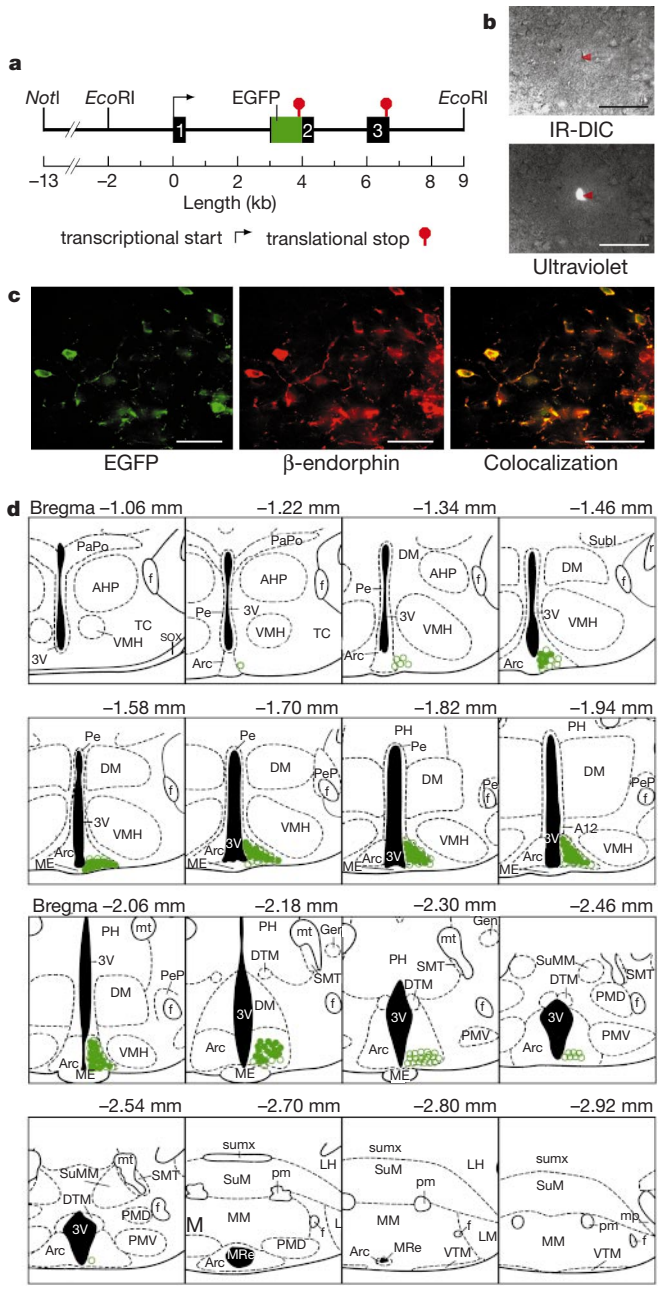

Figure 1 Generation of transgenic mice expressing EGFP in ARC POMC neurons. **a**, Structure of the POMC-EGFP transgene. **b**, Identification of a single POMC neuron (red arrowhead on recording electrode tip) by infrared-differential interference contrast (IR-DIC) microscopy (upper) and EGFP fluorescence (lower) in a living ARC slice before electrophysiological recordings. **c**, Colocalization (yellow) of EGFP (green) and β-endorphin immunoreactivity (red) in ARC POMC neurons. Scale bars, 50 μm (**b**, **c**). **d**, Distribution of EGFP-positive neuronal soma throughout the ARC nucleus. Green open circles = 5 cells, green filled circles = 10 cells.

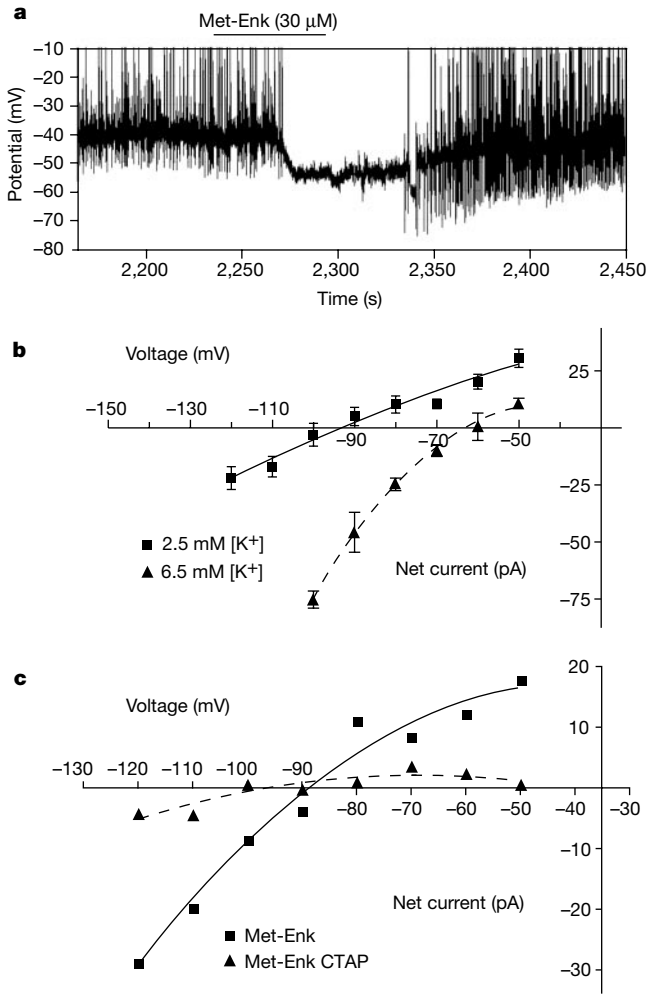

Figure 2 Activation of MOP-Rs hyperpolarizes the EGFP-labelled POMC neurons by opening G-protein-coupled inwardly rectifying potassium channels. **a**, Met-enkephalin (Met-Enk) hyperpolarizes POMC neurons and inhibits all action potentials. Horizontal bar indicates the time when 30 μM Met-Enk was bath applied to the slice. **b**, Met-Enk current and reversal potential is shifted by extracellular K^+ concentration. **c**, Met-Enk activates MOP-Rs on POMC neurons. A Met-Enk (30 μM) current was observed, and the MOP-R-specific antagonist CTAP (1 μM) was applied for 1 min. After CTAP, Met-Enk elicited no current. Figure is representative of three experiments.

mouse[20] POMC cells, identified by post-recording immunohistochemistry, suggests that expression of the EGFP transgene does not compromise expression of receptors nor their coupling to second messenger systems in POMC neurons.

We next determined the direct effects of leptin on identified POMC cells in slice preparations. Leptin (0.1–100 nM) depolarized 72 out of 77 POMC cells by 3–30 mV (Fig. 3a; depolarization at 100 nM leptin, 9.7 ± 1.2 mV (mean ± s.e.m.; $n = 45$)) in 2–10 min, in a concentration-responsive manner (Fig. 3b). There were two components to the depolarization and neither were fully reversible within 40 min. First, the depolarization was due to a small inward current that reversed at about −20 mV (Fig. 3c), suggesting the involvement of a nonspecific cation channel[21]. Second, leptin treatment decreased the GABA-mediated tone onto POMC cells. GABA-mediated inhibitory postsynaptic currents (IPSCs) were observed in POMC cells, and leptin (100 nM) decreased their frequency by 25% (Fig. 3d) in 5 out of 15 cells, indicating that it may act presynaptically to reduce GABA release (leptin had no effect on IPSCs in 10 out of 15 POMC neurons).

The effect on IPSC frequency occurred with a similar lag to the effect on membrane potential. Thus, leptin not only directly depolarizes POMC neurons but also acts at GABA-secreting nerve terminals to reduce the release of GABA onto POMC neurons, allowing them to adopt a more depolarized resting potential. The consistent depolarization of POMC cells by leptin was specific because leptin had no effect on 5 out of 13 adjacent non-fluorescent cells tested (Fig. 3e), whereas it hyperpolarized five (Fig. 3f) and depolarized three other non-POMC neurons in the ARC (data not shown). The electrophysiological effects of leptin reported here are consistent with leptin's biological actions—leptin rapidly causes release of α-melanocyte-stimulating hormone (α-MSH) from rat hypothalami[4], presumably by activating POMC neurons.

Previous reports of neuronal hyperpolarization by leptin[11,12] and the colocalization of GABA and NPY[22] in subpopulations of ARC neurons led us to speculate that leptin hyperpolarizes NPY/GABA cells that directly innervate POMC neurons, and thus reduces GABA-mediated drive onto POMC cells. Both leptin and NPY Y2 receptors are expressed on NPY neurons in the ARC[7,23]. Furthermore, activation of Y2 receptors inhibits NPY release from NPY neurons[24], and presumably would also diminish GABA release from NPY/GABA terminals. This provided us with an alternative pharmacological approach, independent of leptin, to test the proposed innervation of POMC neurons by GABA-secreting NPY neurons.

Indeed, NPY (100 nM; Bachem) decreased the frequency of GABA-mediated IPSCs by 55% in 3 min in all 12 POMC cells tested (Fig. 4a). Both NPY and leptin still inhibited IPSCs in the presence of tetrodotoxin (TTX; 6/6 and 3/5 cells, respectively), indicating that some of the inhibition of IPSCs was occurring through direct effects at presynaptic nerve terminals. POMC neurons express the NPY Y1 receptor[23], and NPY also hyperpolarized all POMC neurons tested by an average of 9 ± 6 mV ($n = 3$; data not shown).

To confirm the origin of GABA-mediated innervation on POMC neurons from NPY/GABA terminals, we also tested the effect of the highly selective MC3-R agonist D-Trp^8-γMSH (ref. 25) on local GABA release. D-Trp^8-γMSH (7 nM) increased the frequency of GABA-mediated IPSCs (280 ± 90%) recorded from three out of four POMC neurons (Fig. 4b). It had no effect on one cell. The positive effect of MC3-R activation, together with the negative effects of NPY and leptin, shows the dynamic range of the NPY/GABA synapse onto POMC neurons and points to the important role of this synapse in modulating signal flow in the ARC. D-Trp^8-γMSH (7 nM) also hyperpolarized (−5.5 ± 2.4 mV) 9 out of 15 POMC neurons tested, and decreased the frequency of action potentials (Fig. 4c); the remaining cells showed no significant response to D-Trp^8-γMSH. We could not determine whether these effects were entirely due to increased GABA release onto the POMC cells, or whether there was an additional postsynaptic action of D-Trp^8-γMSH on POMC neurons, roughly half of which also express the MC3-R[15]. Thus, MC3-R acts in a similar autoreceptor manner to MOP-Rs on POMC neurons, diminishing POMC neuronal activity in response to elevated POMC peptides.

To determine that the IPSCs in POMC neurons were due to local innervation by NPY/GABA cells, we carried out multi-label immuno-

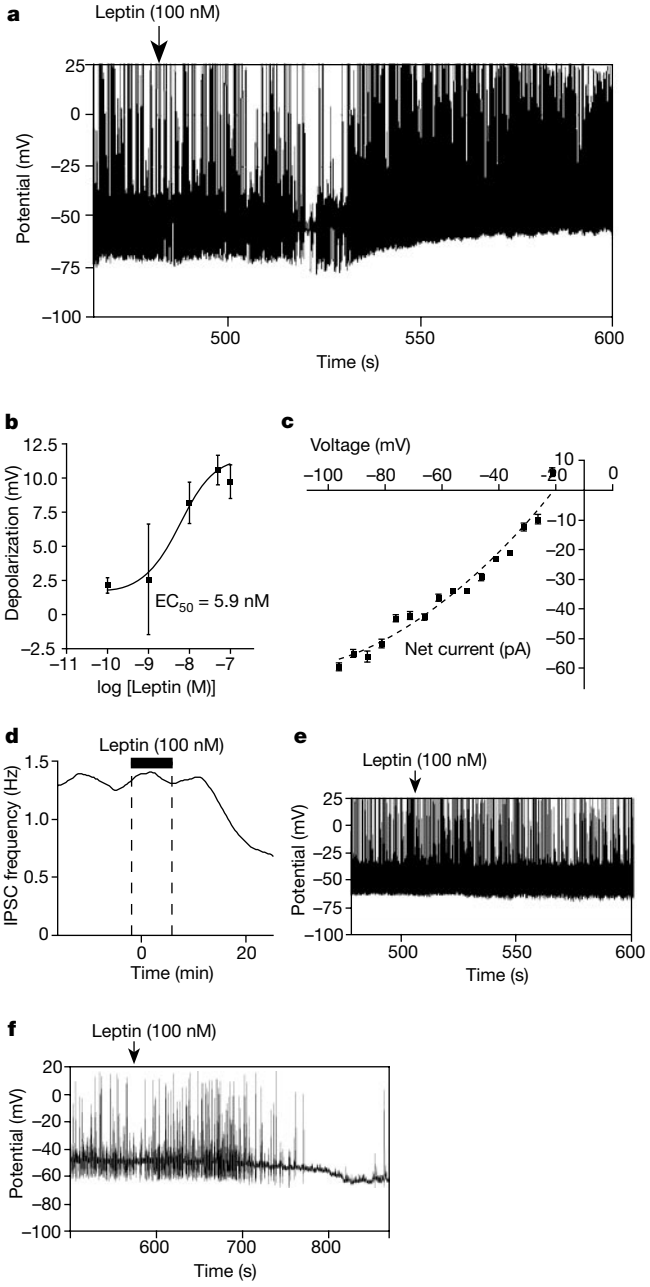

Figure 3 Leptin depolarizes POMC neurons through a nonspecific cation channel, and decreases the GABA-mediated tone onto POMC cells. **a**, Leptin depolarizes POMC neurons and increases the frequency of action potentials within 1–10 min of addition. Figure is representative of recordings made from 77 POMC neurons. **b**, Leptin causes a concentration-dependent depolarization of POMC cells. Depolarization by leptin was determined at 0.1, 1, 10, 50 and 100 nM (effector concentration at half-maximum response, $EC_{50} = 5.9$ nM) in 8, 7, 9, 3 and 45 cells, respectively. **c**, Leptin depolarizes POMC cells by activating a nonspecific cation current. Figure is representative of the response in ten cells. **d**, Leptin decreases the frequency of IPSCs in POMC cells. Figure is an example of five cells in which leptin (100 nM) decreased the frequency of IPSCs. **e**, Leptin had no effect on five adjacent non-fluorescent ARC neurons. **f**, Leptin hyperpolarized five non-fluorescent ARC neurons.

histochemistry using light and electron microscopy. Although independent NPY[27] and GABA[27] innervation of POMC cells has been reported, colocalization of NPY and GABA in nerve terminals forming synapses onto POMC cells has not been shown. Similar to the rat[26], a dense innervation of POMC cells by NPY axon terminals was detected in the mouse (Fig. 4d). Electron microscopy confirmed the co-expression of NPY and GABA in axon terminals, and showed that these boutons established synapses on the perikarya of all 15 ARC POMC neurons analysed (Fig. 4e).

These observations allow us to propose a detailed model of regulation of this circuit including: dual mechanisms of leptin action in the ARC, interactions between NPY/GABA and POMC neurons, and autoregulatory feedback from opioid and melanocortin peptides as well as NPY (Fig. 4f). In this model, leptin directly depolarizes the POMC neurons while simultaneously hyperpolarizing the somata of NPY/GABA neurons, and diminishes release from NPY/GABA terminals. This diminished GABA release disinhibits the POMC neurons. Together, the direct and indirect effects of leptin result in an activation of POMC neurons and an increased frequency of action potentials. In addition, both POMC and NPY neurons express autoreceptors for some of their respective neuropeptide products (β-endorphin or α-MSH, and NPY, respectively) and activation of these autoreceptors may provide ultrashort feedback loops that further modulate the effects of leptin on POMC neurons. The effects of NPY and melanocortin agonists on IPSC frequency are similar to the effect of NPY on IPSCs in the paraventricular nucleus of the hypothalamus[28].

Thus, there seem to be two classes of neurons accounting for leptin sensitivity in the brain: those activated (depolarized) to release anorexigenic peptides; and those inhibited (hyperpolarized) with a consequent reduction in release of orexigenic peptides. Identifying viable POMC neurons with EGFP provides an invaluable tool for determining complex actions on these important neurons. Furthermore, an understanding of the acute effects of leptin provides a model system for studying the mechanisms underlying the development of leptin resistance[29]. □

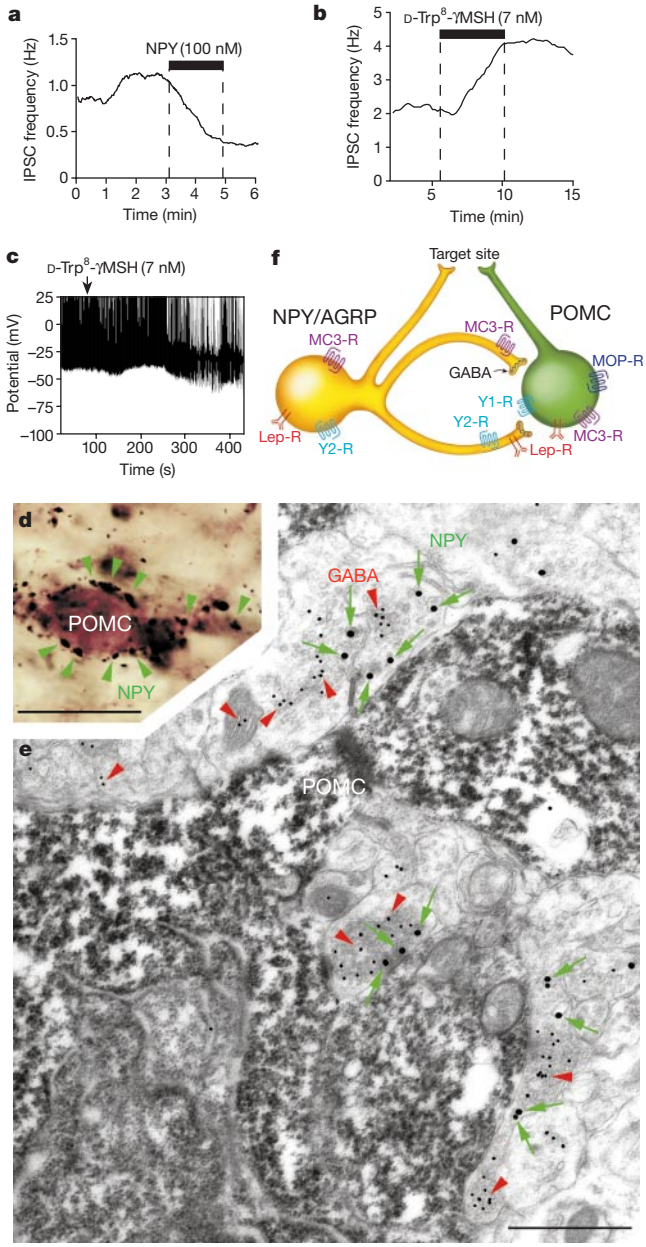

Figure 4 The GABA-mediated inputs to POMC cells are from NPY neurons that co-express GABA. **a**, NPY decreases the frequency of mini-IPSCs in POMC neurons. **b**, D-Trp^8-γMSH (7nM)—a dose that selectively activates MC3-R—increases the frequency of GABA-mediated IPSCs in POMC neurons. **c**, D-Trp^8-γMSH hyperpolarizes POMC neurons. Panels **a**–**c** are representative results. **d**, Expression of NPY in nerve terminals adjacent to POMC neurons in the ARC. NPY nerve terminals (black, green arrowheads); POMC neuronal soma (brown). Scale bar, 10 μm. **e**, Expression of GABA and NPY in nerve terminals synapsing onto POMC neurons in the ARC. GABA immunoreactivity (10-nm gold particles, red arrowheads) and NPY immunoreactivity (25-nm gold particles, green arrows) are in separate vesicle populations colocalized in synaptic boutons that make direct contact with the soma of POMC neurons (DAB contrasted with uranyl acetate and lead citrate, diffuse black in cytoplasm). Scale bar, 1 μm. **f**, Model of leptin regulation of NPY/GABA and POMC neurons in the ARC (see text).

Methods

Generation of POMC-EGFP mice

The *EGFP* cassette contains its own Kozak consensus translation initiation site, along with *SV40* polyadenylation signals downstream of the *EGFP* coding sequences, which directs proper processing of the 3′ end of the EGFP mRNA. We introduced the *EGFP* cassette by standard techniques into the 5′ untranslated region of exon 2 of a mouse *Pomc* genomic clone containing 13 kb of 5′ and 2 kb of 3′ flanking sequences[17]. The transgene was microinjected into pronuclei of one-cell-stage embryos of C57BL/6J mice (Jackson Laboratories) as described[17]. One founder was generated and bred to wild-type C57BL/6J to produce N_1 hemizygous mice. In addition, we also generated N_2 and subsequent generations of mice homozygous for the transgene. The mice are fertile and have normal growth and development.

Immunofluorescence and GFP colocalization

Anaesthetized mice were perfused transcardially with 4% paraformaldehyde, and free-floating brain sections were prepared with a vibratome. We processed sections for immunofluoresence and colocalization of GFP fluoresence using standard techniques. Primary antisera and their final dilutions were rabbit anti-β-endorphin, 1:2500 (v/v); rabbit anti-NPY, 1:25,000 (v/v) (Alanex Corp.); rabbit anti-ACTH, 1:2000 (v/v); and mouse anti-TH, 1:1000 (v/v) (Incstar). After rinsing, sections were incubated with 10 mg ml^{-1} biotinylated horse anti-mouse/rabbit immunoglobulin-γ (IgG) (Vector Laboratories) followed by Cy-3 conjugated streptavidin, 1:500 (v/v) (Jackson Immunoresearch Laboratories). Photomicrographs were taken on an Axioscop (Zeiss) using fluoroscein isothiocyanate (FITC) and rhodamine isothiocyanate (RITC) filter sets (Chroma Technology Corp.).

Electrophysiology

We cut 200-μm thick coronal slices from the ARC of 4-week-old male POMC-EGFP mice. Slices were maintained at 35 °C in Krebs solution ((in mM): 126 NaCl, 2.5 KCl, 1.2 $MgCl_2$, 2.4 $CaCl_2.2H_2O$, 1.2 $NaH_2PO_4.H_2O$, 21.4 $NaHCO_3$, 11.1 glucose), and were saturated with 95% O_2 5% CO_2 for 1 h before recordings. Recordings were made in Krebs solution at 35 °C. Slices were visualized on an Axioskop FS2 (Zeiss) through standard infrared optics and using epifluoresence through a FITC filter set (see Fig. 1c). Whole-cell recordings were made from fluorescent neurons using an Axopatch 1D amplifier (Axon Instruments) and Clampex 7 (Axon Instruments).

We determined resting membrane potentials using an event-detection protocol on a PowerLab system (AD Instruments) to average expanded traces of the membrane potential. Drugs were applied to the bath over the times indicated. The resting membrane potential was stable for up to 1 h in cells treated with Krebs solution alone (data not shown). *I–V* relationships for the Met-Enk currents were established using a step protocol (−60 mV holding potential, sequentially pulsed (40 ms) from −120 to −50 mV; cells were returned to −60 mV for 2 s between voltage steps). The protocol was repeated after addition of Met-Enk. The net current was the difference between the two *I–V* relation-

ships. This protocol was repeated in Krebs solution with 6.5 mM K^+. To identify the postsynaptic leptin current, *I–V* relationships were performed similarly with slow voltage ramps (5 mV s^{-1} from −100 to −20 mV) before and 10 min after adding leptin (100 nM).

GABA-mediated IPSCs were recorded using a CsCl internal electrode solution ((in mM): 140 CsCl, 10 HEPES, 5 $MgCl_2$, 1 BAPTA, 5 Mg-ATP, 0.3 Na-GTP). Both mini IPSCs and large amplitude (presumably multisynaptic) IPSCs were observed in the untreated slices. TTX (1 μM) abolished large IPSCs. We acquired data before and after drug addition at a −50-mV holding potential in 2-s sweeps every 4 s for the times indicated in the figures. Mini-postsynaptic currents were analysed using Axograph 4 (Axon Instruments). IPSCs and excitatory postsynaptic currents (EPSCs) were distinguished on the basis of their decay constants; in addition, picrotoxin (100 μM) blocked all IPSCs. POMC neurons receive a low EPSC tone, and the frequency was not modulated by any of the treatments described here.

Immunostaining for light and electron microscopy

We carried out double immunocytochemistry for NPY and POMC using different colour diaminobenzidine (DAB) chromogens on fixed mouse hypothalami according to published protocols[27]. For electron microscopy, pre-embedding immunostaining for β-endorphin was done with an ABC Elite kit (Vector Laboratories) and a DAB reaction, followed by post-embedding labelling of GABA and NPY using rabbit anti-GABA, 1:1000 (v/v), and gold-conjugated (10-nm) goat anti-rabbit IgG or sheep anti-NPY and gold-conjugated (25-nm) goat anti-sheep IgG. Sections were contrasted with saturated uranyl acetate (10 min) and lead citrate (20–30 s), and examined using a Philips CM-10 electron microscope.

Received 19 December 2000; accepted 12 March 2001.

1. Zhang, Y. *et al.* Positional cloning of the mouse obese gene and its human homologue. *Nature* **372,** 425–432 (1994); erratum *ibid.* **374,** 479 (1995).
2. Farooqi, I. S. *et al.* Effects of recombinant leptin therapy in a child with congenital leptin deficiency. *N. Engl. J. Med.* **341,** 879–884 (1999).
3. Campfield, L. A., Smith, F. J., Guisez, Y., Devos, R. & Burn, P. Recombinant mouse OB protein: evidence for a peripheral signal linking adiposity and central neural networks. *Science* **269,** 546–549 (1995).
4. Kim, M. S. *et al.* The central melanocortin system affects the hypothalamo-pituitary thyroid axis and may mediate the effect of leptin. *J. Clin. Invest.* **105,** 1005–1011 (2000).
5. Haynes, W. G., Morgan, D. A., Walsh, S. A., Mark, A. L. & Sivitz, W. I. Receptor-mediated regional sympathetic nerve activation by leptin. *J. Clin. Invest.* **100,** 270–278 (1997).
6. Haynes, W. G., Morgan, D. A., Djalali, A., Sivitz, W. I. & Mark, A. L. Interactions between the melanocortin system and leptin in control of sympathetic nerve traffic. *Hypertension* **33,** 542–547 (1999).
7. Hakansson, M. L., Brown, H., Ghilardi, N., Skoda, R. C. & Meister, B. Leptin receptor immunoreactivity in chemically defined target neurons of the hypothalamus. *J. Neurosci.* **18,** 559–572 (1998).
8. Kalra, S. P. *et al.* Interacting appetite-regulating pathways in the hypothalamic regulation of body weight. *Endocr. Rev.* **20,** 68–100 (1999).
9. Cone, R. D. The central melanocortin system and energy homeostasis. *Trends Endocrinol. Metab.* **10,** 211–216 (1999).
10. Elias, C. F. *et al.* Leptin differentially regulates NPY and POMC neurons projecting to the lateral hypothalamic area. *Neuron* **23,** 775–786 (1999).
11. Glaum, S. R. *et al.* Leptin, the obese gene product, rapidly modulates synaptic transmission in the hypothalamus. *Mol. Pharmacol.* **50,** 230–235 (1996).
12. Spanswick, D., Smith, M. A., Groppi, V. E., Logan, S. D. & Ashford, M. L. Leptin inhibits hypothalamic neurons by activation of ATP-sensitive potassium channels. *Nature* **390,** 521–525 (1997).
13. Lee, K., Dixon, A. K., Richardson, P. J. & Pinnock, R. D. Glucose-receptive neurones in the rat ventromedial hypothalamus express KATP channels composed of Kir6.1 and SUR1 subunits. *J. Physiol. (Lond.)* **515,** 439–452 (1999).
14. Shiraishi, T., Sasaki, K., Niijima, A. & Oomura, Y. Leptin effects on feeding-related hypothalamic and peripheral neuronal activities in normal and obese rats. *Nutrition* **15,** 576–579 (1999).
15. Bagnol, D. *et al.* Anatomy of an endogenous antagonist: relationship between Agouti-related protein and proopiomelanocortin in brain. *J. Neurosci.* [online] (cited 25 Aug. 99) <http://www.jneurosci.org/cgi/content/full/19/18/RC26> (1999).
16. Butler, A. A. *et al.* A unique metabolic syndrome causes obesity in the melanocortin-3 receptor-deficient mouse. *Endocrinology* **141,** 3518–3521 (2000).
17. Young, J. I. *et al.* Authentic cell-specific and developmentally regulated expression of pro-opiomelanocortin genomic fragments in hypothalamic and hindbrain neurons of transgenic mice. *J. Neurosci.* **18,** 6631–6640 (1998).
18. Franklin, K. B. J. & Paxinos, G. *The Mouse Brain in Stereotaxic Coordinates* (Academic, San Diego, 1997).
19. Kelly, M. J., Loose, M. D. & Ronnekleiv, O. K. Opioids hyperpolarize β-endorphin neurons via μ-receptor activation of a potassium conductance. *Neuroendocrinology* **52,** 268–275 (1990).
20. Slugg, R. M., Hayward, M. D., Ronnekleiv, O. K., Low, M. J. & Kelly, M. J. Effect of the μ-opioid agonist DAMGO on medial basal hypothalamic neurons in β-endorphin knock-out mice. *Neuroendocrinology* **72,** 208–217 (2000).
21. Powis, J. E., Bains, J. S. & Ferguson, A. V. Leptin depolarizes rat hypothalamic paraventricular nucleus neurons. *Am. J. Physiol.* **274,** R1468–R1472 (1998).
22. Horvath, T. L., Bechmann, I., Naftolin, F., Kalra, S. P. & Leranth, C. Heterogeneity in the neuropeptide Y-containing neurons of the rat arcuate nucleus: GABAergic and non-GABAergic subpopulations. *Brain Res.* **756,** 283–286 (1997).
23. Broberger, C., Landry, M., Wong, H., Walsh, J. N. & Hokfelt, T. Subtypes Y1 and Y2 of the neuropeptide Y receptor are respectively expressed in pro-opiomelanocortin- and neuropeptide-Y-containing neurons of the rat hypothalamic arcuate nucleus. *Neuroendocrinology* **66,** 393–408 (1997).
24. King, P. J., Widdowson, P. S., Doods, H. N. & Williams, G. Regulation of neuropeptide Y release by neuropeptide Y receptor ligands and calcium channel antagonists in hypothalamic slices. *J. Neurochem.* **73,** 641–646 (1999).
25. Grieco, P., Balse, P. M., Weinberg, D., MacNeil, T. & Hruby, V. J. D-Amino acid scan of gamma-melanocyte-stimulating hormone: importance of Trp(8) on human MC3 receptor selectivity. *J. Med. Chem.* **43,** 4998–5002 (2000).
26. Csiffary, A., Gorcs, T. J. & Palkovits, M. Neuropeptide Y innervation of ACTH-immunoreactive neurons in the arcuate nucleus of rats: a correlated light and electron microscopic double immunolabeling study. *Brain Res.* **506,** 215–222 (1990).
27. Horvath, T. L., Naftolin, F. & Leranth, C. GABAergic and catecholaminergic innervation of mediobasal hypothalamic beta-endorphin cells projecting to the medial preoptic area. *Neuroscience* **51,** 391–399 (1992).
28. Cowley, M. A. *et al.* Integration of NPY, AGRP, and melanocortin signals in the hypothalamic paraventricular nucleus: evidence of a cellular basis for the adipostat. *Neuron* **24,** 155–163 (1999).
29. Halaas, J. L. *et al.* Physiological response to long-term peripheral and central leptin infusion in lean and obese mice. *Proc. Natl Acad. Sci. USA* **94,** 8878–8883 (1997).

Acknowledgements

We wish to thank V. J. Hruby for the D-Trp^8-γMSH, O. K. Ronnekliev, R. G. Allen and M. R. Brown for antisera and J. T. Williams and J. M. Brundege for advice. This work was supported by the NIH, a Fogarty International Research Collaborative Award, the International Scholar Program of the Howard Hughes Medical Institute, and Agencia Nacional de Promoción Cientifica y Technológica.

Correspondence and requests for materials should be addressed to R.D.C. (e-mail: cone@ohsu.edu) or M.J.L. (e-mail: low@ohsu.edu).

Calmodulin bifurcates the local Ca^{2+} signal that modulates P/Q-type Ca^{2+} channels

Carla D. DeMaria*, Tuck Wah Soong†, Badr A. Alseikhan*, Rebecca S. Alvania* & David T. Yue*

* *The Johns Hopkins University School of Medicine, Departments of Biomedical Engineering and Neuroscience, Program in Molecular and Cellular Systems Physiology, 720 Rutland Avenue, Baltimore, Maryland 21205, USA*
† *National Neuroscience Institute, 11 Jalan Tan Tuck Seng, Singapore 308433, and Department of Physiology, National University of Singapore*

Acute modulation of P/Q-type (α_{1A}) calcium channels by neuronal activity-dependent changes in intracellular Ca^{2+} concentration may contribute to short-term synaptic plasticity[1–3], potentially enriching the neurocomputational capabilities of the brain[4,5]. An unconventional mechanism for such channel modulation has been proposed[6,7] in which calmodulin (CaM) may exert two opposing effects on individual channels, initially promoting ('facilitation') and then inhibiting ('inactivation') channel opening. Here we report that such dual regulation arises from surprising Ca^{2+}-transduction capabilities of CaM. First, although facilitation and inactivation are two competing processes, both require Ca^{2+}-CaM binding to a single 'IQ-like' domain on the carboxy tail of α_{1A}[8]; a previously identified 'CBD' CaM-binding site[6,7] has no detectable role. Second, expression of a CaM mutant with impairment of all four of its Ca^{2+}-binding sites (CaM_{1234}) eliminates both forms of modulation. This result confirms that CaM is the Ca^{2+} sensor for channel regulation, and indicates that CaM may associate with the channel even before local Ca^{2+} concentration rises. Finally, the bifunctional capability of CaM arises from bifurcation of Ca^{2+} signalling by the lobes of CaM: Ca^{2+} binding to the amino-terminal lobe selectively initiates channel inactivation, whereas Ca^{2+} sensing by the carboxy-terminal lobe induces facilitation. Such lobe-specific detection provides a compact means to decode local Ca^{2+} signals in two ways, and to separately initiate distinct actions on a single molecular complex.

To simplify the dissection of the molecular mechanisms, we studied recombinant P/Q-type ($\alpha_{1A}/\beta_{2a}/\alpha_2\delta$) channels expressed in mammalian HEK293 cells. Figure 1a shows that Ca^{2+}-dependent